

Precambrian Palaeolatitudes for Australia

– an update –

prepared for Geoscience Australia

Mart Idnurm

April 2004

Introduction

Palaeolatitudes for Precambrian Australia were last reported in 1988¹. A serious limitation at that time was the sparseness of palaeomagnetic data. While the Australian Precambrian still lacks palaeomagnetic data on the whole, two intervals within it have since become much better defined. These are the late Palaeoproterozoic to earliest Mesoproterozoic and late the Mesoproterozoic to middle Neoproterozoic. Improvements to the former resulted from multidisciplinary studies in the 1990s by AGSO to provide a geological framework for mineral exploration in northern Australia; improvements to the latter are largely due a quest led by the University of Western Australia to determine the configuration of the late Proterozoic supercontinent Rodinia. This report incorporates the improvements in data for an update on Australian Precambrian palaeolatitudes.

Palaeomagnetic determination of palaeolatitudes

The derivation of palaeolatitudes by use of palaeomagnetism is based on the geocentric axial dipole hypothesis – when averaged over time, the geomagnetic field may be represented by that of a magnetic dipole located at the centre of the Earth and aligned along its rotation axis. A period of few thousand years is generally considered sufficient to average out the components in the geomagnetic field that cause it to differ from that of the geocentric axial dipole. Given such a dipole field, the palaeolatitude may be calculated from its inclination at any particular locality using the equation:

$$\tan I = 2 \cot p,$$

where I is the inclination of the field and p is the palaeo-colatitude of the locality.

The inclination of the ancient geomagnetic field is obtained by analysing the magnetic records of rock formations.

The validity of the geocentric axial dipole hypothesis can be tested by using global palaeomagnetic data (for its dipole character) together with palaeoclimatic data (for axial alignment). Such tests confirm that the dipole field was a good approximation of the geomagnetic field during the Phanerozoic². Similar data are not available for the tests in the Precambrian. Therefore, to obtain Precambrian palaeolatitudes, it is necessary to assume that the same processes within the conductive outer liquid core of the Earth which generated the Phanerozoic geomagnetic field had operated in earlier times.

¹ Idnurm, M. and Giddings, J.W., 1988. Australian Precambrian polar wander: a review. *Precambrian Research*, **40/41**, 61-88.

² Merrill, R.T., McElhinny, M.W. and McFadden, P.L., 1996. *The magnetic field of the Earth: Palaeomagnetism, the core, and the deep mantle*. Academic Press, San Diego, 528 pp.

Palaeolatitude database

The palaeomagnetic poles, their geochronological ages and the respective 95% (or alternatively 2sd) uncertainties used in this update are listed in Table 1. Also listed are the rock formations and geological units from which the data were obtained. The Ps and Cs in the References column of the table give the sources of the palaeomagnetic (P) geochronological (C) data. Some palaeomagnetic poles used in the 1988 summary have since been contested, and are therefore omitted. These include the poles for the Gawler Range Volcanics³ and a Yilgarn dykes suite (YE)⁴.

Palaeolatitude vs time diagrams

Figure 1 shows the variation of palaeolatitude in time with Alice Springs taken as the reference locality. A detail for the interval 1.8 – 1.6 Ga in which the plot is particularly well defined is shown in Fig. 1a. The Precambrian structural units from where the palaeolatitudes were obtained are coded by colour. Error bars in the diagrams indicate 95% (or 2sd) confidence limits. It is possible that the Precambrian units were not assembled in their present-day configuration – especially during the Archaean, if not subsequently. If so, a palaeolatitude estimate would be valid for only that unit (and any others attached to it) from which the data were obtained. The reference locality would then need to be imagined as a fictitious, or projected, reference point relative to the particular structural unit(s).

Palaeolatitudes may be estimated by interpolation between successive points in the diagrams, provided the gap is not large. Trend lines, or rather bands, are shown in the figures to assist interpolation. The band for the Archaean is highly tentative, pending a substantial increase in data.

A disadvantage of the palaeolatitude-time diagrams is that each applies only to a particular reference locality. Palaeolatitudes of other localities may differ substantially, depending on their distance from the reference locality and on the orientation of the continent relative to the geographic pole. This is illustrated in Fig. 2 where palaeolatitudes for Alice Springs (23.7°S, 133.9°E) are compared with those of the Tanami mine (20.0°S, 129.7°E) approximately 600 km to the northwest. The palaeolatitude difference ranges from -5° to +5°.

³ P.W. Schmidt quoted in: Idnurm, M., Giddings, J.W. and Plumb, K.A., 1995. Apparent polar wander and reversal stratigraphy of the Palaeo-Mesoproterozoic southeastern McArthur Basin, Australia. *Precambrian Research*, **72**, 1-41.

⁴ Halls, H. C. and Wingate, M.T.D., 2001. Paleomagnetic pole from the Yilgarn B (YB) dykes of Western Australia: no longer relevant to Rodinia reconstructions. *Earth and Planet. Sci. Lett.*, **187**, 39-53.

Palaeogeographic diagrams

Figures 3a to 3g show Australia relative to the geographic (strictly, time-averaged palaeomagnetic) pole at 19 different times during the Precambrian. This type of representation overcomes the problem of determining palaeolatitudes of different locations as it allows interpolation between palaeolatitude lines. The diagrams, however, have the drawback that the rate of latitudinal change in the time interval between successive diagrams (palaeogeographic 'snapshots') is not clear, making it difficult to estimate palaeolatitudes for in-between times. The palaeogeographic diagrams also do not convey the sometimes substantial uncertainties in the palaeolatitude estimates. In general, the best approach is to use the time variation and palaeogeographic diagrams in conjunction, while keeping in mind that the Australian Precambrian units may not have been in their present day configuration.

Table 1. Palaeomagnetic poles used in palaeolatitude determination

Structural unit and rock formation	Pole Latitude deg. N	Pole Longitude deg. E	A95 dp, dm deg.	Age Ga	Reference	Pole Acronym	Pallat. Alice Spr. deg. N	Pallat. Tanami deg. N
<i>Adelaide Geosyncline</i>								
Elatina Formation	-52.4	347.1	3.7,7.4	.65-.60	P1,C1	EF	8.6	10.6
Bunjeroo Formation	-18.1	16.3	6.5,11.8	0.59	P2,C2	BF	16.2	14.4
<i>Amadeus Basin</i>								
Pertatataka Formation, Ringwood Mbr	-65	278	8,15	.73+/- .05	P3,C3	PR	-2.9	1.6
<i>Arunta Block</i>								
Stuart Dykes	10	262	10	1.06+/- .04	P4,C4	SD	38.8	43
<i>Gawler Block</i>								
GA dykes	-61	51	9	1.47+/- .20	P5,C5	GA	-24	-22.9
<i>Hammersley Basin</i>								
Mount Roe Basalt	52	358	6,9	~2.8	P6,C6	RB	46.2	40.9
<i>Kimberley Block</i>								
Hart Dolerite	-29	226	24	1.790+/- .004	P7,C7	HD	-9.5	-4.3
Elgee Formation	-4.4	210	3.3,6.5	1.704+ .007/- .014	P8,C8	LG	-14.5	-10.6
<i>McArthur Basin</i>								
Hobblechain Rhyolite	-17.6	209.9	11.9	1.725+/- .002	P9,C9	HR	-19.4	-14.8
West Branch Volcanics	-15.9	200.5	11.3	1.709+/- .010	P10,C10	WBV	-27.4	-23
Amos Formation	-66.5	178.4	4.5	1.614+/- .004	P11,C11	AFB	-39	-34.1
Balberini Dolomite, lower	-66.1	177.5	5.7	1.609+/- .003	P12,C12	BDBL	-39.5	-34.6
Balberini Dolomite, upper	-52	176.1	7.5	1.589+/- .003	P13,C13	BDBU	-47.3	-42
Lynott Formation	-75.1	162.8	6.2	1.636+/- .004	P14,C14	LYN	-36.5	-32.2
Lynott Formation	21.5	78.3	5.9		P14a,C14a	LYNO		
Tatoola Sandstone	-52.7	182.2	10.7	1.648+/- .003	P15,C15	TAT	-43.5	-38.2
Wollogorang Formation	-17.9	218.2	7.2	1.730+/- .003	P16,C16	WFK	-12.1	-7.4
<i>Mount Isa Block</i>								
Lakeview Dolerite	9.5	311.1	17.4	1.116+/- .012	P17,C17	IAR	75.6	79.4
Peters Creek Volcanics	-26	221	4.8	1.724+/- .002	P18,C18	PCVU	-12.6	-7.5

Table 1. Palaeomagnetic poles used in palaeolatitude determination (cont.)

Structural unit and rock formation	Pole Latitude deg. N	Pole Longitude deg. E	A95 dp,dm deg.	Age Ga	Reference	Pole Acronym	Pallat. Alice Spr. deg. N	Pallat. Tanami deg. N
<i>Musgrave Block</i>								
Giles Complex	18	307	23,29	~1.078	P19,C19	GC	81.4	86.8
Kulgera Dyke Suite	-17	266	12	1.090+/-0.032	P20,C20	KG	28	33.3
<i>Northampton Block</i>								
Basic dykes, Northampton Block	-47.1	317.3	8	.748+/-0.016	P21,C21	NDD	19.1	22.6
<i>Pilbara Block</i>								
Duffer Formation	-44	266	7	3.452+/-0.016	P22,C22	DFM	9.3	14.5
Millindinna Complex	12	341	7,8	2.86+/-0.02	P23,C23	MIL	61.8	58.9
Black Range dyke	32	334	9	>/~ 2.7	P24,C24	BR	70.4	65.2
Mundine dykes, WA	-43.8	314.1	5.1	.755+/-0.003	P25,C25	MDS	21	24.6
<i>Pine Creek Inlier</i>								
Plum Tree Creek Volcanics	-29	195	14	1.825+/-0.004	P34,C34	PTV	-35.6	-30.6
<i>Yilgarn Block</i>								
Ravensthorpe dykes	38	316	26	2.45+/-0.10	P26,C26	RD	75.6	71.2
Widgiemoolta dykes	9	337	8	2.37+/-0.03	P27,C27	WD	63.5	61.4
YE dykes	-28	0	31	~2.45	P28,C28	YE	21	21.7
YF dykes	-25	282	14	~1.66	P29,C29	YF	32.3	37.6
Morawa lavas	20	59	17	1.36+/-0.14	P30,C30	ML	-5	-10.1
<i>Albany-Fraser Mobile Belt</i>								
Bremer Bay & Whalebone Point area	74.4	303.8	12.2,14.7	~1.2	P31,C31	BB1	39	35.5
Mount Barren Group	55.8	325.7	11.9,13.9	~1.2	P32,C32	MBG	56.7	52.2
<i>Bangemall Basin</i>								
Bangemall Basin sediments	-33.8	275	8.3	1.070+/-0.006	P33,C33	BBS	21.6	26.9

Table 1 References

P1 Schmidt, P.W. and Williams, G.E., 1995. The Neoproterozoic climatic paradox: Equatorial palaeolatitude for Marinoan glaciation near sea level in South Australia. *Earth. Planet. Sci. Lett.*, **134**, 107–124.

C1 Age range of 650–600 for Elatina Formation estimated by Schmidt and Williams in *P1*.

P2 Schmidt, P.W. and Williams, G.E., 1996. Palaeomagnetism of the ejecta-bearing Bunyeroo Formation, late Neoproterozoic, Adelaide fold belt, and the age of the Arcaman impact. *Earth. Planet. Sci. Lett.*, **144**, 347–357.

C2 See discussion of Bunyeroo Formation age in *P2*, based on:

- Compston, W., Williams, I.S., Jenkins, R.J.F., Gostin, V.A., and Haines, P.W., 1987. Zircon age evidence for the Late Precambrian Arcaman ejecta blanket. *Aust. J. Earth Sci.*, **34**, 435–445.
- Webb, A.W., Coats, R.P., Fanning, C.M. and Flint, R.B., 1983. Geochronological framework of the Adelaide Geosyncline. *Geol. Soc. Aust. Abstr.*, **10**, 7–9. (*Rb-Sr, poorly defined*)

P3 McWilliams, M.O., 1981. Palaeomagnetism and Precambrian tectonic evolution of Gondwana. In: A. Kröner (ed.), *Precambrian Plate Tectonics, Developments in Precambrian Geology*, **4**. Elsevier, Amsterdam, pp. 649–687.

C3 Compston, W. and Taylor, S.R., 1969. Rb-Sr study of impact glass and country rocks from the Henbury crater field. *Geochimica et Cosmochimica Acta*, **33**, 1037–1043. (*Rb-Sr*)

P4 Idnurm, M and Giddings, J.W., 1988. Australian Precambrian polar wander: A review. *Precambrian Res.*, **40/41**, 61–88.

C4 Zhao, J.-X. and McCulloch, M.T., 1993. Sm-Nd mineral isochron ages of Late Proterozoic dyke swarms in Australia: evidence for two distinctive events of mafic magmatism and crustal extension. *Chem. Geol. (Isot. Geosci. Sect.)*, **109**, 341–354. (*Sm-Nd*)

P5 Giddings, J.W. and Embleton, B.J.J., 1976. Precambrian palaeomagnetism in Australia II: Basic dykes from the Gawler Block. *Tectonophysics*, **30**, 109–118.

C5 Compston W. pers. comm. in *P6*. (*Rb-Sr*)

P6 Schmidt, P.W. and Embleton, B.J.J., 1985. Prefolding and overprint magnetic signatures in Precambrian (2.9–2.7 Ga) igneous rocks from the Pilbara Craton and Hamersley Basin, NW Australia. *J. Geophys. Res.*, **90**, 2967–2984.

C6 Gulson, B.L. and Korsch, M.J., 1983. Isotope studies, *Bien. Rep.* 1981/82, pp. 24–26. CSIRO Div. Min. Phys., Sydney. (*Sm-Nd and Pb-Pb*)

P7 McElhinny, M.W. and Evans, M.E., 1976. Palaeomagnetic results from the Hart Dolerite of the Kimberley Block, Australia. *Precambrian Res.*, **3**, 231–241.

C7 Geoscience Australia OZCHRON database sample 87598003 (*SHRIMP U-Pb zircon*).

P8 Li, Z.-X., 2000. Palaeomagnetic evidence for unification of the North and West Australian Cratons by ca. 1.7 Ga: new results from the Kimberley Basin of northwestern Australia. *Geophys. J. Int.*, **142**, 173–180.

C8 McNaughton, N.J., Rasmussen, B. and Fletcher, I.R., 1999. SHRIMP uranium-lead dating of diagenetic xenotime in siliciclastic sedimentary rocks. *Science*, **285**, 78–80. (*SHRIMP U-Pb xenotime*)

P9 Idnurm, M., Giddings, J.W. and Plumb, K.A., 1995. Apparent polar wander and reversal stratigraphy of the Palaeo-Mesoproterozoic southeastern McArthur Basin, Australia. *Precambrian Res.*, **72**, 1–41.

C9 Page, R.W., Jackson, M.J. and Krassay, A.A., 2000. Constraining sequence stratigraphy in north Australian basins: SHRIMP U-Pb zircon geochronology between Mt Isa and McArthur River. *Aust. J. Earth Sci.*, **47**, 431–459. (*SHRIMP U-Pb zircon*)

P10 Idnurm, M., 2000. Towards a high resolution Late Palaeoproterozoic – earliest Mesoproterozoic apparent polar wander path for northern Australia. *Aust. J. Earth Sci.*, **47**, 405–429.

C10 Kruse, P.D., Sweet, I.P., Stuart-Smith, P.G., Wygralak, A.S. Pieters, P.E and Crick, I.H., 1994. Katherine 1:250 000 Geological Map Series. Northern Territory Geological Survey, Explanatory Notes **SD53-9**. (*SHRIMP U-Pb zircon*)

P11 Idnurm, M., 2000. Towards a high resolution Late Palaeoproterozoic – earliest Mesoproterozoic apparent polar wander path for northern Australia. *Aust. J. Earth Sci.*, **47**, 405–429.

C11 Page, R.W., Jackson, M.J. and Krassay, A.A. 2000. Constraining sequence stratigraphy in north Australian basins: SHRIMP U-Pb zircon geochronology between Mt Isa and McArthur River. *Aust. J. Earth Sci.*, **47**, 431–459. (*SHRIMP U-Pb zircon*)

P12 Idnurm, M., 2000. Towards a high resolution Late Palaeoproterozoic – earliest Mesoproterozoic apparent polar wander path for northern Australia. *Aust. J. Earth Sci.*, **47**, 405–429.

C12 Page, R.W., Jackson, M.J. and Krassay, A.A. 2000. Constraining sequence stratigraphy in north Australian basins: SHRIMP U-Pb zircon geochronology between Mt Isa and McArthur River. *Aust. J. Earth Sci.*, **47**, 431–459. (*SHRIMP U-Pb zircon*)

P13 Idnurm, M., 2000. Towards a high resolution Late Palaeoproterozoic – earliest Mesoproterozoic apparent polar wander path for northern Australia. *Aust. J. Earth Sci.*, **47**, 405–429.

C13 Page, R.W., Jackson, M.J. and Krassay, A.A. 2000. Constraining sequence stratigraphy in north Australian basins: SHRIMP U-Pb zircon geochronology between Mt Isa and McArthur River. *Aust. J. Earth Sci.*, **47**, 431–459. (*SHRIMP U-Pb zircon*)

P14 Idnurm, M., 2000. Towards a high resolution Late Palaeoproterozoic – earliest Mesoproterozoic apparent polar wander path for northern Australia. *Aust. J. Earth Sci.*, **47**, 405–429.

C14 Page, R.W., Jackson, M.J. and Krassay, A.A. 2000. Constraining sequence stratigraphy in north Australian basins: SHRIMP U-Pb zircon geochronology between Mt Isa and McArthur River. *Aust. J. Earth Sci.*, **47**, 431–459. (*SHRIMP U-Pb zircon*)

P14a Idnurm, M., 2000. Towards a high resolution Late Palaeoproterozoic – earliest Mesoproterozoic apparent polar wander path for northern Australia. *Aust. J. Earth Sci.*, **47**, 405–429.

C14a This is an undated magnetic overprint. Its pole position on the APWP suggests an age between 1.6 and 1.5 Ga.

P15 Idnurm, M., 2000. Towards a high resolution Late Palaeoproterozoic – earliest Mesoproterozoic apparent polar wander path for northern Australia. *Aust. J. Earth Sci.*, **47**, 405–429.

C15 Page, R.W., Jackson, M.J. and Krassay, A.A. 2000. Constraining sequence stratigraphy in north Australian basins: SHRIMP U-Pb zircon geochronology between Mt Isa and McArthur River. *Aust. J. Earth Sci.*, **47**, 431–459. (*SHRIMP U-Pb zircon*)

P16 Idnurm, M., 2000. Towards a high resolution Late Palaeoproterozoic – earliest Mesoproterozoic apparent polar wander path for northern Australia. *Aust. J. Earth Sci.*, **47**, 405–429.

C16 Page, R.W., Jackson, M.J. and Krassay, A.A. 2000. Constraining sequence stratigraphy in north Australian basins: SHRIMP U-Pb zircon geochronology between Mt Isa and McArthur River. *Aust. J. Earth Sci.*, **47**, 431–459. (*SHRIMP U-Pb zircon*)

P17 Tanaka, H. and Idnurm, M., 1994. Palaeomagnetism of Proterozoic mafic intrusions and host rocks of the Mount Isa Inlier Australia: revisited. *Precambrian Res.*, **69**, 241–258.

C17a (Rb-Sr) Page, R., 1983. Chronology of magmatism, skarn formation, and uranium mineralization, Mary Kathleen, Queensland, Australia. *Econ. Geol.*, **78**, 838–853.

C17b Unpublished. (*Shrimp U-Pb baddelyite*)

P18 Idnurm, M., 2000. Towards a high resolution Late Palaeoproterozoic – earliest Mesoproterozoic apparent polar wander path for northern Australia. *Aust. J. Earth Sci.*, **47**, 405–429.

C18 Page, R.W., Jackson, M.J. and Krassay, A.A. 2000. Constraining sequence stratigraphy in north Australian basins: SHRIMP U-Pb zircon geochronology between Mt Isa and McArthur River. *Aust. J. Earth Sci.*, **47**, 431–459. (*SHRIMP U-Pb zircon*)

- P19* Facer, R.A., 1971. Magnetic properties of rocks from the Giles Complex, central Australia. *J. Proc. Roy. Soc. N.S.W.*, **104**, 45–61. (Pole calculation error corrected by Tanaka, H. and Idnurm, M., 1994. Palaeomagnetism of Proterozoic mafic intrusions and country rocks of the Mt Isa Inlier, Australia. *Precambrian Research*, **69**, 241–258.)
C19 Glikson, A.Y., Stewart, A.J., Ballhaus, C.G., Clarke, G.L., Feeken, E.H.J., Leven, J.H., Sheraton, J.W. and Sun, S-S, 1996. Geology of the western Musgrave Block, central Australia, with particular reference to the mafic-ultramafic Giles Comple. *Australian Geological Society Organisation Bulletin*, **239**. (*U-Pb zircon and Pb-Pb give an age estimate for this overprint*)
- P20* Camacho, A., Simons, B. and Schmidt, P.W., 1991. Geological and palaeomagnetic significance of the Kulgera Dyke Swarm, Musgrave Block, NT, Australia. *Geophys. Res. Int.*, **107**, 37–45.
C20 Zhao, J.-X. and McCulloch, M.T., 1993. Sm-Nd mineral isochron ages of Late Proterozoic dyke swarms in Australia: evidence for two distinctive events of mafic magmatism and crustal extension. *Chem. Geol. (Isot. Geosci. Sect.)*, **109**, 341–354. (*Sm-Nd*)
- P21* Embleton, B.J.J. and Schmidt, P.W., 1985. Age and significance of magnetizations of dolerite dykes from the Northampton Block, Western Australia. *Aust. J. Earth Sci.*, **32**, 279–286.
C21 Wingate and Giddings (P25) reinterpretation of the geochronology reported in P21, (*K-Ar*)
- P22* McElhinny M.W. and Senanayake, W.E., 1980. Palaeomagnetic evidence for the existence of the geomagnetic field 3.5 Ga ago. *J. Geophys. Res.*, **85**, 3523–3528.
C22 Pidgeon, R.T., 1978. 3450-m.y.-old volcanics in the Archaean layered greenstone succession of the Pilbara Block, Western Australia. *Earth Planet. Sci. Lett.*, **37**, 421–428. (*U-Pb zircon*)
- P23* Schmidt, P.W. and Embleton, B.J.J. 1985. Prefolding and overprint magnetic signatures in the Precambrian (2.9–2.7 Ga) igneous rocks from the Pilbara Craton and Hamersley Basin, NW Australia. *J. Geophys. Res.*, **90**, 2967–2984.
C23 Gulson, B.L. and Korsch, M.J., 1983. Isotope studies, *Bien. Rep.* 1981/82, pp. 24-26. CSIRO Div. Min. Phys., Sydney. (*Sm-Nd, Pb-Pb*)
- P24* Embleton, B.J.J., 1978. The palaeomagnetism of 2400 m.y. rocks from the Australian Pilbara Craton and its relation to Archaean-Proterozoic tectonics. *Precambrian Res.*, **6**, 275–291.
C24 J.R. de Laeter, pers. comm. (1984) in P23.
- P25* Wingate, M.T.D and Giddings, J.W., 2000. Age and palaeomagnetism of the Mundine Well dyke swarm, Western Australia: Implications for an Australia-Laurentia connection at 755 Ma. *Precambrian Res.*, **100**, 335-357.
C25 as P25. (*SHRIMP U-Pb zircon and baddeleyite*)
- P26* Giddings, J.W., 1976. Precambrian palaeomagnetism in Australia I: Basic dykes and volcanics from the Yilgarn Block. *Tectonophysics*, **30**, 91–108.
C26 W. Compston and Crawford, pers. comm., in P26 (preliminary date). (*Rb-Sr*)
- P27* Evans, M.E., 1968. Magnetization of dykes: A study of the palaeomagnetism of the Widgiemooltha Dike Suite, Western Australia. *J. Geophys. Res.*, **73**, 3261–3270.
C27 Turek, A., 1966. Rubidium-strontium isotopic studies in the Kalgoorlie-Norseman area, Western Australia, Ph.D. thesis, Australian National University, Canberra. (*Rb-Sr*)
- P28* Giddings, J.W., 1976. Precambrian palaeomagnetism in Australia I: Basic dykes and volcanics from the Yilgarn Block. *Tectonophysics*, **30**, 91–108.
C28 W. Compston and Crawford, pers. comm., in P26 (preliminary date). (*Rb-Sr*)
- P29* Giddings, J.W., 1976. Precambrian palaeomagnetism in Australia I: Basic dykes and volcanics from the Yilgarn Block. *Tectonophysics*, **30**, 91–108.
C29 W. Compston and Crawford, pers. comm., in P26 (preliminary date). (*Rb-Sr*)

P30 Idnurm, M and Giddings, J.W., 1988. Australian Precambrian polar wander: A review. *Precambrian Res.*, **40/41**, 61–88.

C30 P.A. Arriens unpublished information, reported in *P29*. (*Rb-Sr*)

P31 Pisarevsky, S.A., Wingate, M.T.D. and Harris, L.B., 2003. Late Mesoproterozoic (ca 1.2 Ga) palaeomagnetism of the Albany-Fraser orogen: no pre-Rodinia Australia-Laurentia connection. *Geophys. J. Int.*, **155**, F6–F11.

C31 Indirect age, interpreted in *P31* as due to tectonothermal events in the Albany and Fraser Mobile Belts, based on:

- Black, L.P., Harris, L.B. and Delor, C.P., 1992. Reworking of Archaean and Early Proterozoic components during a progressive, Middle Proterozoic tectonothermal event in the Albany Mobile Belt, Western Australia. *Precambrian Res.*, **59**, 95–123 (*U-Pb zircon*).
- Dawson, G.C., Krapez, B., Fletcher, I.R., McNaughton, N.J. and Rasmussen, B., 2003. 1.2 Ga thermal metamorphism in the Albany-Fraser Orogen of Western Australia: consequences of collision or regional heating by dyke swarms? *J. Geol. Soc. Lond.*, **160**, 29–37 (*SHRIMP u-Pb xenotime and monazite*).

P32 Pisarevsky, S.A., Wingate, M.T.D. and Harris, L.B., 2003. Late Mesoproterozoic (ca 1.2 Ga) palaeomagnetism of the Albany-Fraser orogen: no pre-Rodinia Australia-Laurentia connection. *Geophys. J. Int.*, **155**, F6–F11.

C32 Indirect age, interpreted in *P32* as due to tectonothermal events in the Albany and Fraser Mobile Belts, based on:

- Black, L.P., Harris, L.B. and Delor, C.P., 1992. Reworking of Archaean and Early Proterozoic components during a progressive, Middle Proterozoic tectonothermal event in the Albany Mobile Belt, Western Australia. *Precambrian Res.*, **59**, 95–123 (*U-Pb zircon*).
- Dawson, G.C., Krapez, B., Fletcher, I.R., McNaughton, N.J. and Rasmussen, B., 2003. 1.2 Ga thermal metamorphism in the Albany-Fraser Orogen of Western Australia: consequences of collision or regional heating by dyke swarms? *J. Geol. Soc. Lond.*, **160**, 29–37 (*SHRIMP u-Pb xenotime and monazite*).

P33 Wingate, M.T.D., Pisarevsky, S.A. and Evans, D.A.D., 2002. New palaeomagnetic constraints on Rodinia connections between Australia and Laurentia. *GSA Abstracts with Programs*, **34**, 559.

C33 Reported also in *P33*. (*SHRIMP U-Pb baddeleyite*)

P34 Idnurm, M. and Giddings, J.W., 1988. Australian Precambrian polar wander: A review. *Precambrian Res.*, **40/41**, 61–88.

C34 Kruse, P.D., Sweet, I.P., Stuart-Smith, P.G., Wygralak, A.S. Pieters, P.E and Crick, I.H., 1994. Katherine 1:250 000 Geological Map Series. Northern Territory Geological Survey, Explanatory Notes **SD53–9**. (*SHRIMP U-Pb zircon*)

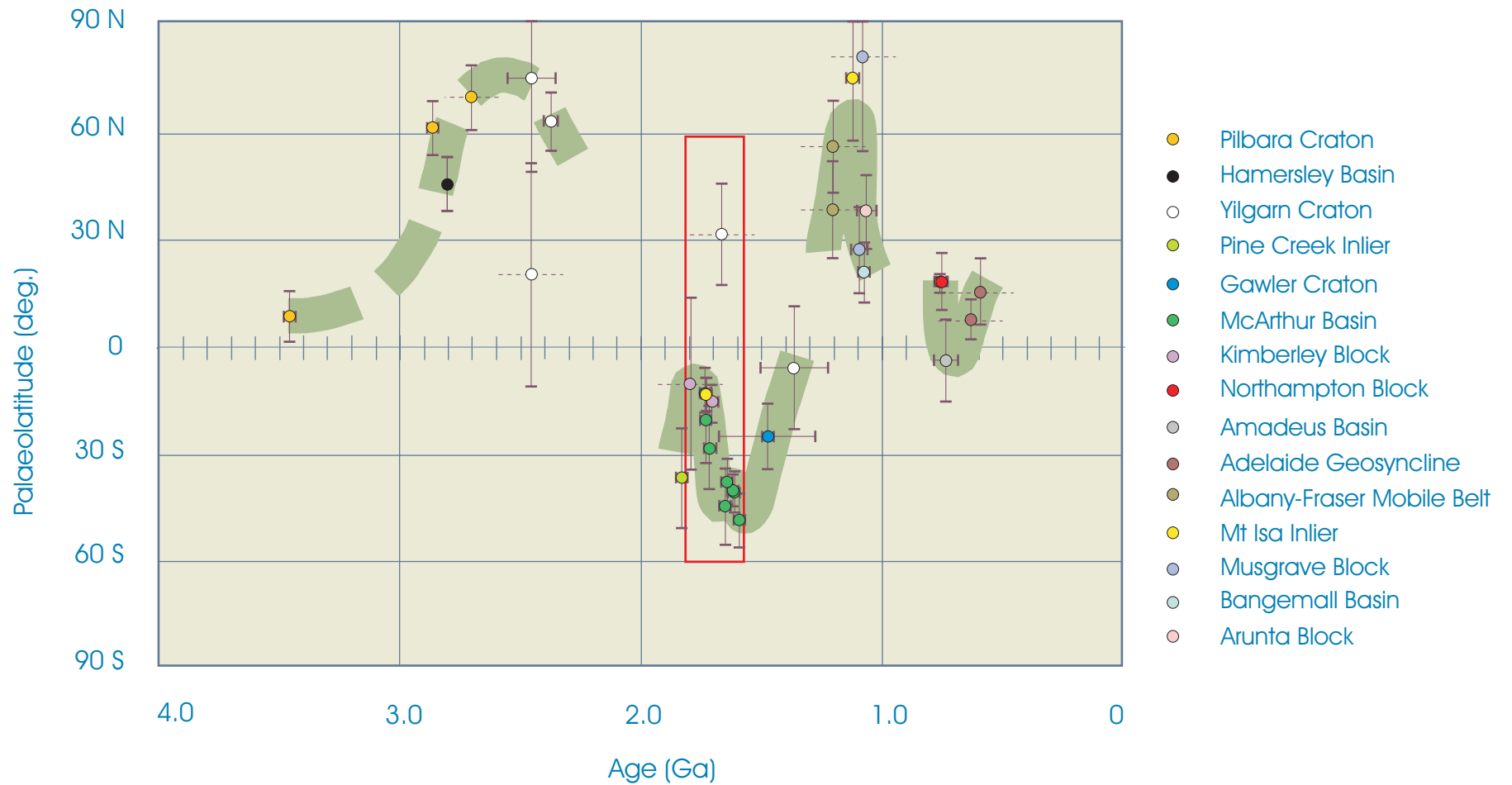


Fig.1 Precambrian palaeolatitudes for Australia with Alice Springs as the reference locality. 95% (or 2sd) confidence intervals are shown in solid lines. Broken lines signify approximate ages. Area in rectangle is expanded in Fig. 1a.



Fig.1a Detail of Fig.1 for the interval 1.8 to 1.6 Ga.

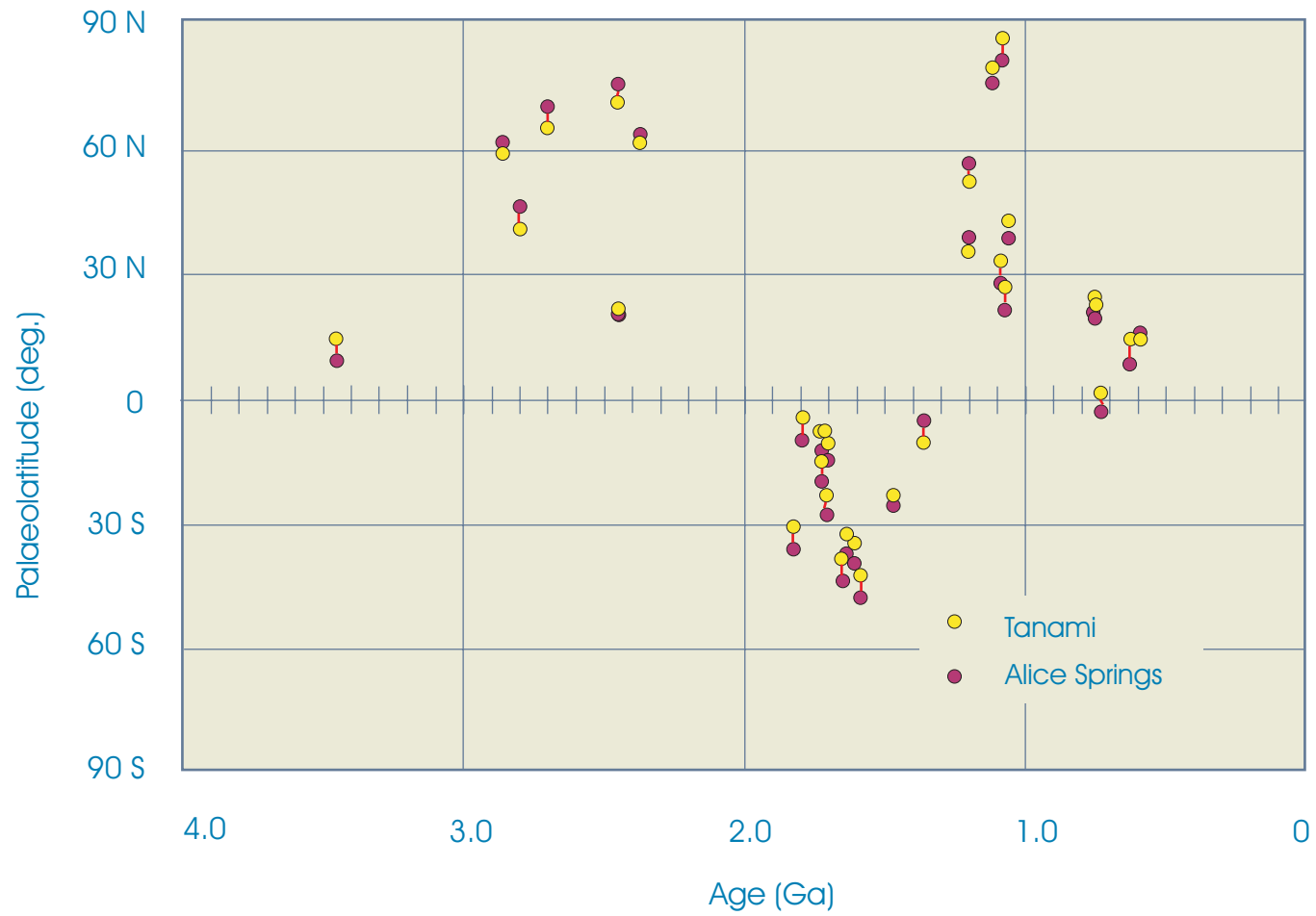


Fig.2 Comparison of palaeolatitudes of Alice Springs and the Tanami mine. Corresponding palaeolatitudes that differ by more than a few degrees are shown linked.

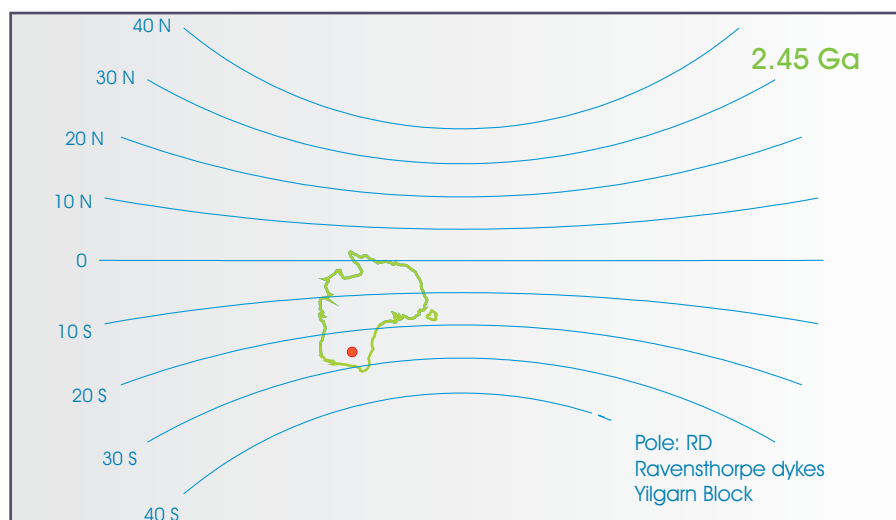
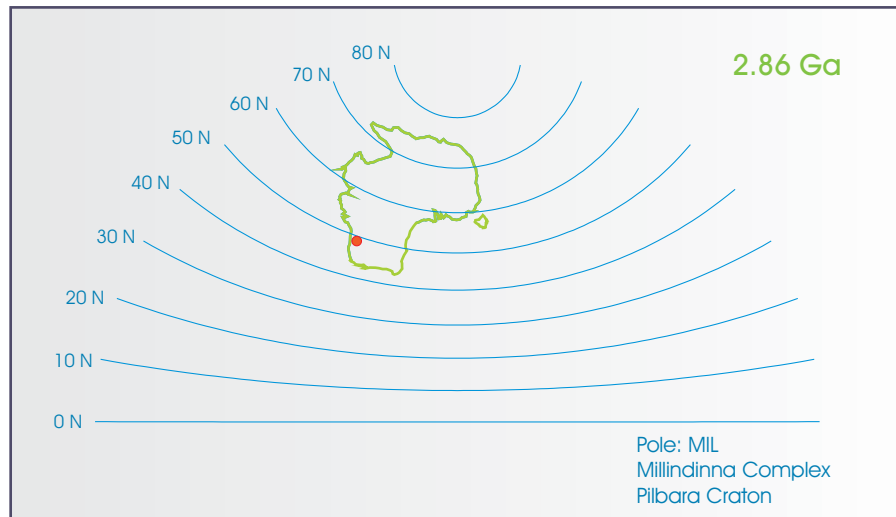
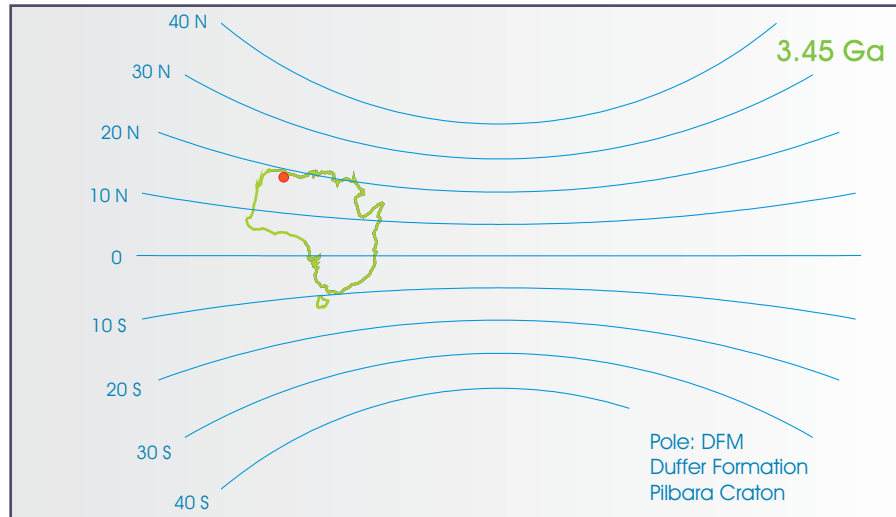


Fig. 3a Figs.3a - 3g show palaeolatitudes of various Australian structural units (located by red dots) during the Precambrian.

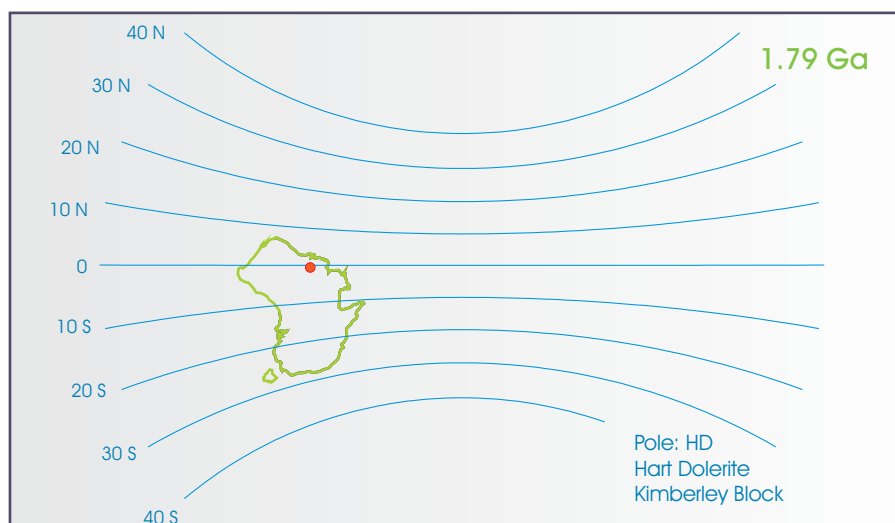
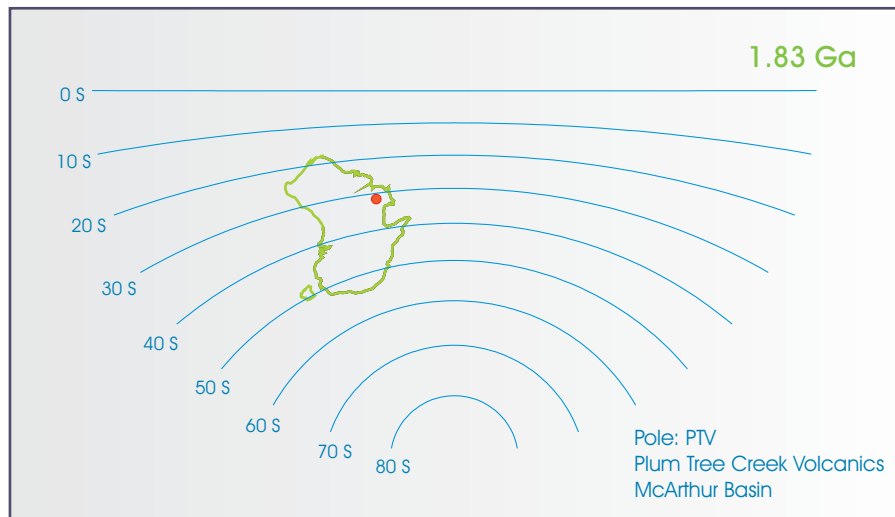
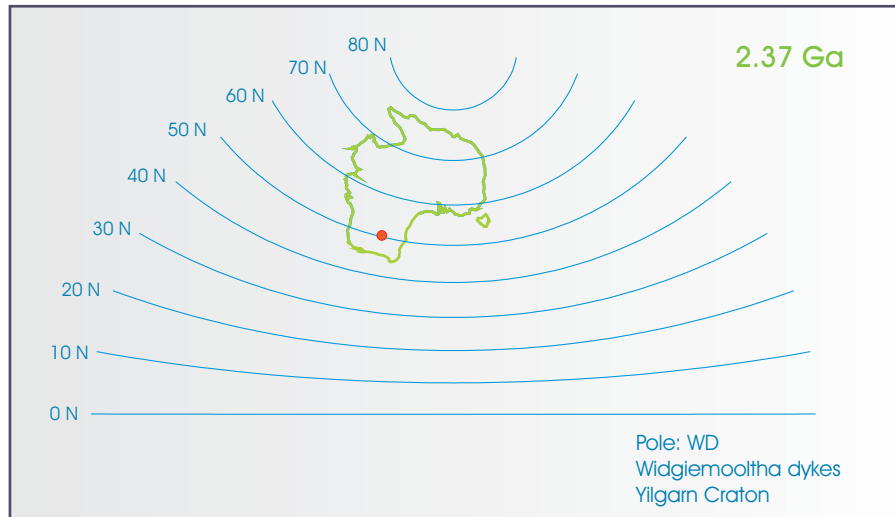


Fig. 3b

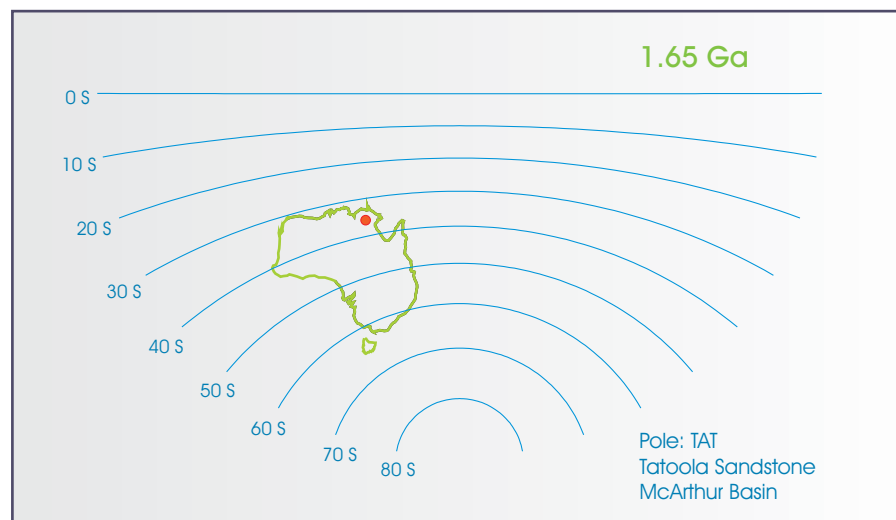
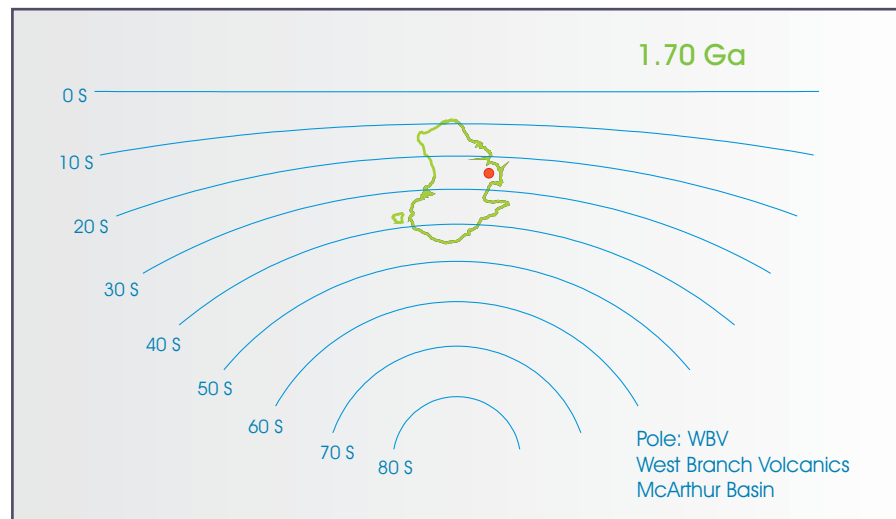
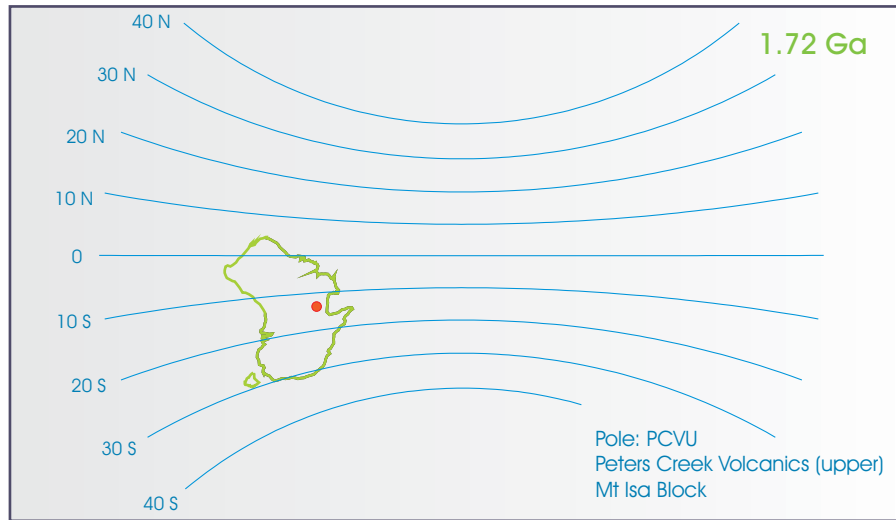


Fig. 3c

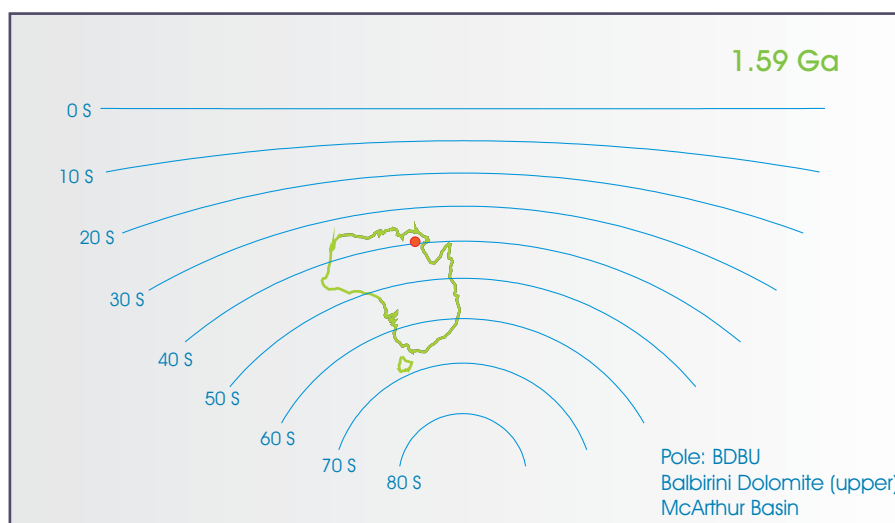
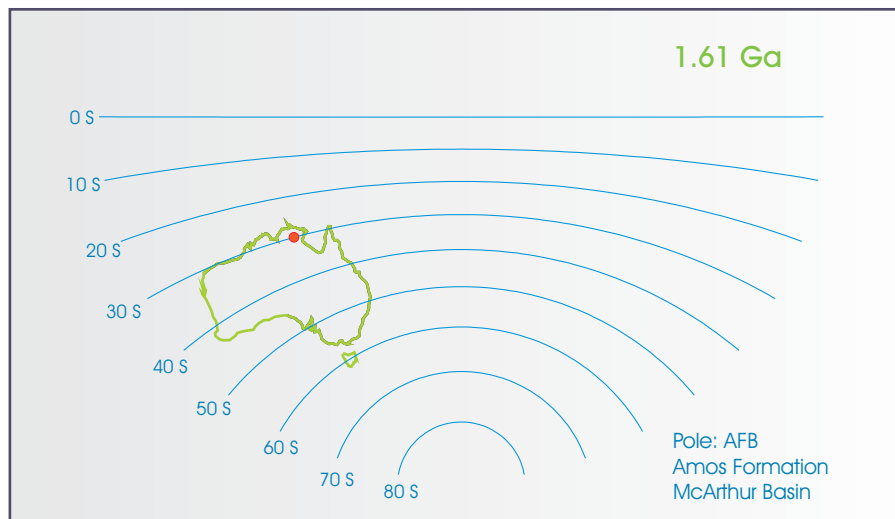
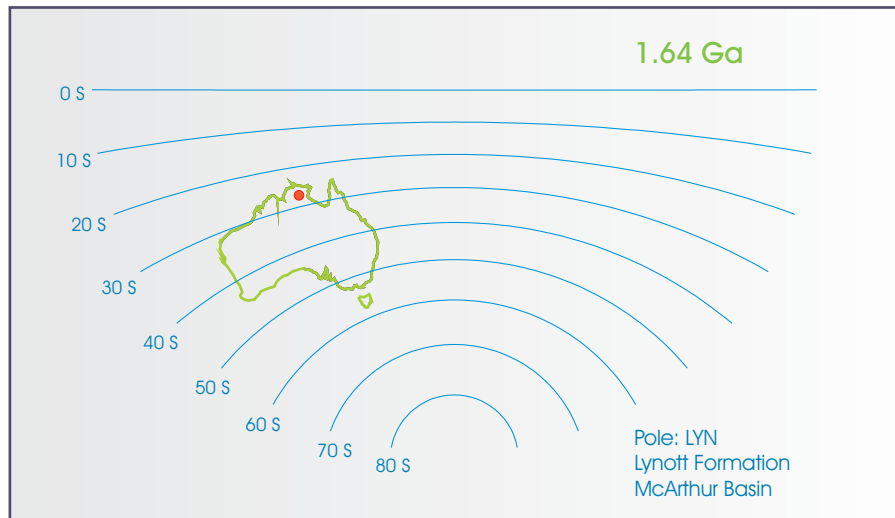


Fig. 3d

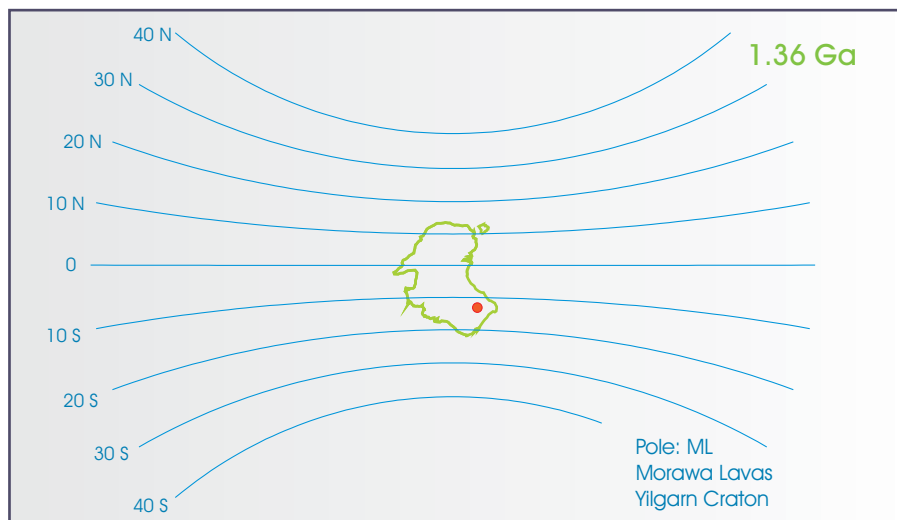
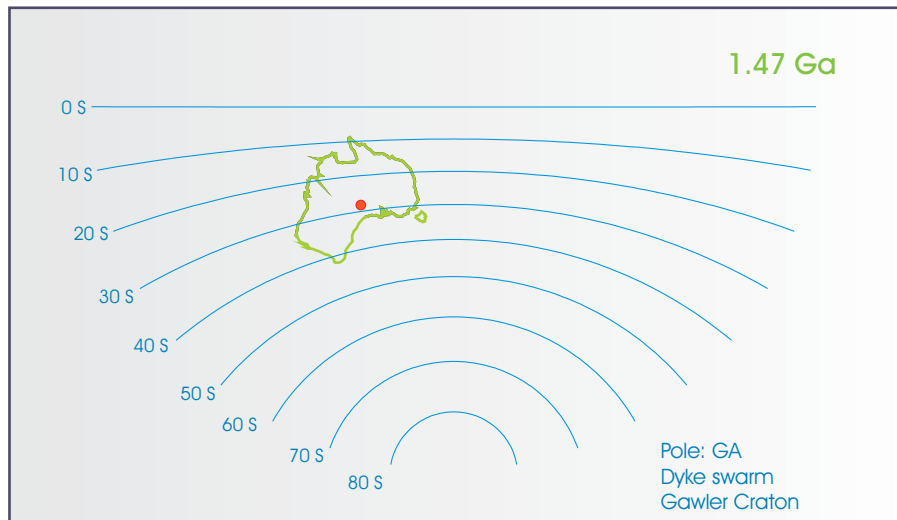
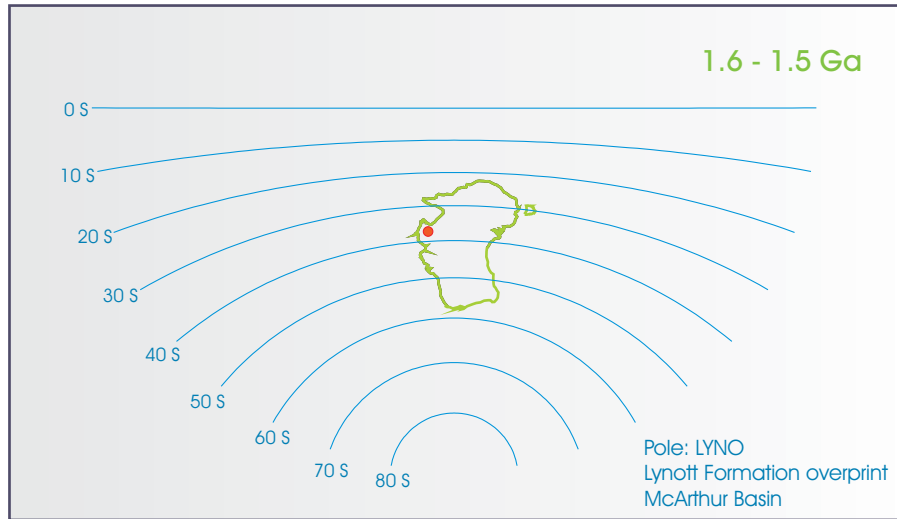


Fig. 3e

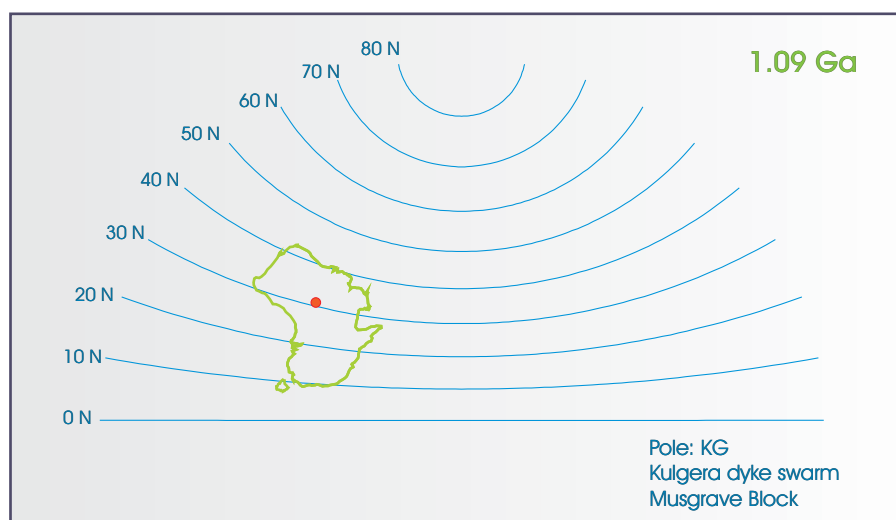
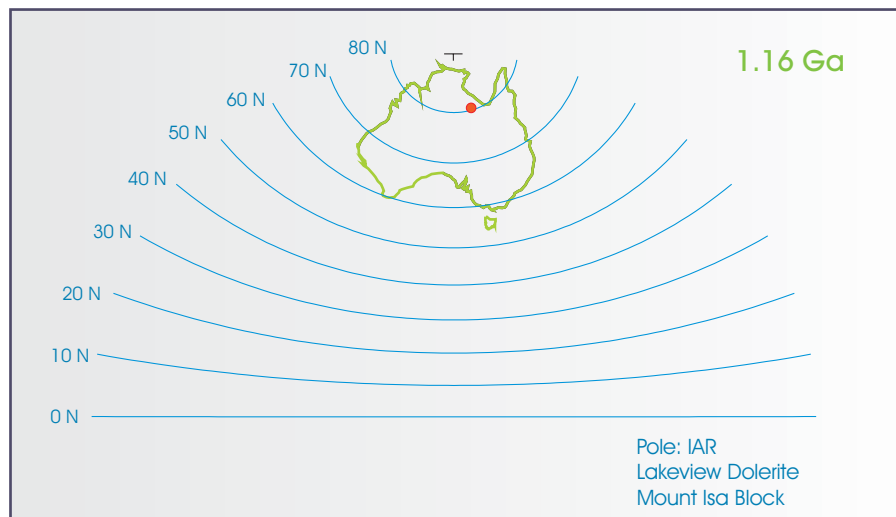
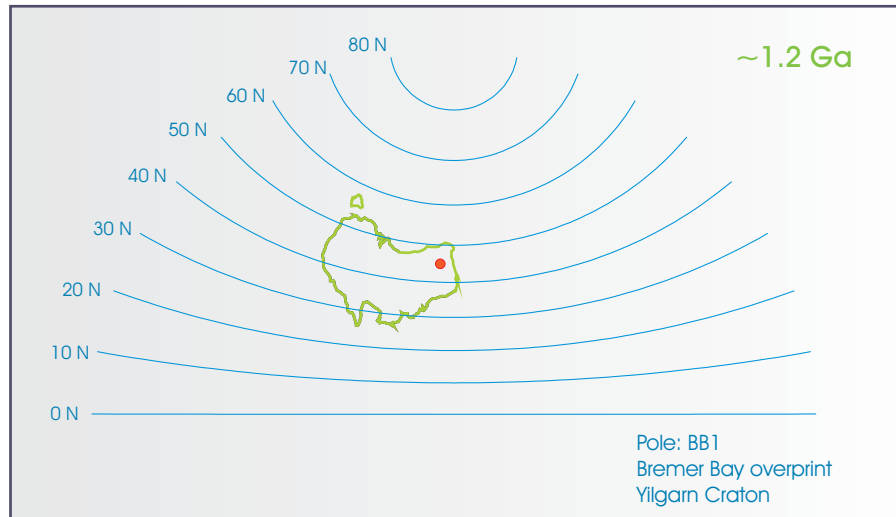


Fig. 3f



Fig. 3g